Angewandte Chemie
Eine Zeitschrift der Gesellschaft Deutscher Chemiker

Supporting Information

Promoting the Electrocatalytic Performance of Noble Metal Aerogels by Ligand-Directed Modulation

Xuelin Fan, Swen Zerebecki, Ran Du, René Hübner, Galina Marzum, Guocan Jiang, Yue Hu, Stephan Barcikowki, Sven Reichenberger, and Alexander Eychmüller**

anie_201913079_sm_miscellaneous_information.pdf

Experimental Procedures

Reagents and Materials

Reagents including sodium borohydride ($NaBH_4$), trisodium citrate dihydrate (NaCA), polyvinylpyrrolidone (PVP, M_w = 58000), cetyltrimethyl ammonium bromide (CTAB), 20 wt.% palladium on carbon, and others were purchased from Sigma-Aldrich or Alfa-Aesar. All reagents are used without further purification.

Fabrication of Noble Metal Nanoparticles (NPs)

Colloidal Au NPs and Pd NPs were prepared by pulsed laser ablation in liquid (PLAL) in 1 mM NaOH aqueous solution. Therefore, a pulsed Nd:YAG laser (EdgeWave IS-400-L) with a wavelength of 1064 nm, a repetition rate of 5 kHz, a pulse energy of ~12 mJ, and a pulse duration of 8 ns was used. The laser was focused through an F-Theta lens (LINOS, f = 100) on a 1 mm thick Pd or Au foil (99.99% AGOSI) inside a self-build continuous flow chamber (similar to ref. 1). The laser spot was moved at 2 m s^{-1} in a circular pattern over the foil by a galvanometric scanner system (Sunny S-8210D). The NaOH solution was pumped (pump Ismatec ISM321C) through the chamber with a flow rate of 100 mL min^{-1} until a concentration of 100–125 mg L^{-1} was reached equal to a productivity of ~0.6 g h^{-1}. The nanoparticle mass was determined by weighing the target prior and after ablation using a microbalance (PESA Weighing Systems) with 10 µg accuracy. Afterwards, the particle size of the obtained colloids was reduced to < 10 nm by pulsed laser fragmentation in liquid (PLFL) using a ps-laser system (EdgeWave SN 1056, wavelength: 355 nm, repetition rate: 50 kHz, pulse energy: 0.2 mJ). Here, the colloid was released through a modified funnel (diameter of funnel opening and the liquid jet: 0.5 mm) while the laser was focused with a cylinder lens (f = 75 mm) onto the liquid jet (similar to ref. 2). The distance between cylinder lens and the liquid jet was 70 mm.

Fabrication of Noble Metal Hydrogels (NMHs)

Hydrogels were synthesized by a $NaBH_4$-induced gelation. As an example, the fabrication of the Au-Pd gel is demonstrated. The Au and Pd NP solutions were mixed together and diluted with deionized water, giving rise to a concentration of 0.25 mM for both metals. Then freshly prepared $NaBH_4$ aqueous solution (1.0 M, 250.0 µL) was added to the mixed NP solution (4.75 mL) under stirring. After grounding for ~12 h, a monolithic gel was obtained. The fabrication process can be readily scaled up to 800 mL with the same procedure.

Fabrication of Noble Metal Aerogels (NMAs)

The as-prepared hydrogels were washed by a large amount of water for 4–5 times with a total duration of 2–3 days to remove possible residues. To load the specific ligands, the hydrogels were further exchanged with the ligand solution (0.1 M) for three times, then they were washed with water to remove the weakly adsorbed ligands. Afterwards, the resulting hydrogels were flash-freezed by liquid nitrogen and remained at −196 ºC for ~10 min to enable complete freezing, then they were freeze-dried at ~1 Pa for 12–24 h.

Characterizations

Microscopy Characterization

Scanning electron microscopy (SEM) analysis was performed on a Zeiss Gemini 500 scanning electron microscope. Samples were prepared by directly sticking on conductive tape.

Transmission electron microscopy (TEM) analysis was carried out by using a FEI Tecnai G2 20 or a JEM-2100F microscope operated at 200 kV. Samples were prepared by dispersing in acetone under ultrasonication (15 s to 120 s, depending on their dispersing ability), followed by dropping onto carbon-coated copper grids and drying at ambient temperature.

High-angle annular dark-field scanning transmission electron microscopy (HAADF-STEM) imaging and spectrum imaging based on energy-dispersive X-ray spectroscopy (EDX) were performed at 200 kV with a Talos F200X microscope equipped with an X-FEG electron source and a Super-X EDX detector system (FEI). Prior to STEM analysis, the specimen mounted in a high-visibility low-background holder was placed for 2 s into a Model 1020 Plasma Cleaner (Fischione) to remove possible contamination.

Diffraction Characterization

X-ray powder diffraction (XRD) was carried out in reflection mode on a Siemens D5000 X-ray diffractometer operated at a voltage of 30 kV and a current of 10 mA with Cu Kα radiation (λ = 1.5406 Å). The data were collected in the range of 20°–90° (2θ) with a step size of $\Delta 2\theta = 0.02°$. The sample was fixed on the holder by Scotch tape.

Size Distribution Analysis

The hydrodynamic particle size was analyzed by analytical disc centrifugation (DC24000, CPS Instrument) at 24 000 rpm for 20 min against a saccharose gradient and an external standard (Au particles at 7 nm), using a sample volume of 0.1 mL. Also for some indicated places, TEM statistics were used for analyzing the size distribution.

Spectroscopy Characterization

Ultraviolet–visible spectroscopy (UV-vis) absorption spectra were recorded on a Cary 60 UV-Vis Spectrophotometer.

Raman spectra were recorded on a Renishaw's inVia microscope, where an excitation wavelength of 532 nm and an integration time of 60 s were adopted.

Element Analysis

X-ray photoelectron spectroscopy (XPS) was performed on an Axis Ultra spectrometer (Kratos, UK) with a high-performance Al monochromatic source operated at 15 kV. The XPS spectra were taken after all binding energies were referenced to the C 1s neutral carbon peak at 284.8 eV, and the elemental compositions were determined from the peak area ratios after correction with the sensitivity factors from CasaXPS.

Inductively coupled plasma optical emission spectroscopy (ICP-OES) was performed on a Perkin-Elmer Optima 7000DV optical emission spectrometer.

Gas Adsorption Measurement

Nitrogen adsorption experiments were performed with a Quantachrome NOVA 3000e system at 77 K. The sample was outgassed at 323 K for ~24 h under vacuum before measurement. The filling rod was used to reduce the dead volume, thus improving the measurement accuracy. The specific surface area was calculated by using the multi-point BET equation ($0.1 < p/p_0 < 0.3$). The pore size distribution was derived by using the non-local density functional theory (NLDFT) method (N_2 at 77 K on carbon) based on a slit pore geometry. The total pore volume was calculated at $p/p_0 = 0.99$, similar to the value derived by the BJH (Barret–Joyner–Halender) method.

Electrochemical Measurements

All electrochemical tests were performed with a three-electrode system on an Autolab/PGSTAT 30 (Eco Chemie B. V. Utrecht, the Netherlands) or a CHI potentiostat (CHI 760D). A glassy carbon electrode (GCE, 3 mm in diameter), an Ag/AgCl (saturated KCl aqueous solution) electrode, and a platinum foil were used as working electrode, reference electrode, and counter electrode, respectively. For modification of the working electrode, ~1.0 mg catalyst was dispersed in 425 μL 2-propanol (IPA) and 75 μL Nafion (1 wt.% in IPA) by sonicating for ca. 30 min to acquire the catalyst ink. Then a specific amount of ink was transferred on the GCE and evaporated at ambient temperature. The concentration of Pd in the ink was determined by ICP-OES, and the total loading of Pd was calculated accordingly to ~20 μg cm^{-2}.

Before all tests, CV was performed in 1.0 M KOH aqueous solution for several tens of cycles to stabilize the electrode materials, until the curves remained unchanged. For the electro-oxidation of ethanol, the test was performed under N_2 atmosphere in 1.0 M KOH aqueous solution containing 1.0 M ethanol. CV curves were recorded between –0.9 and 0.3 V (*vs.* AgCl/Ag) with a scanning rate of 50 mV s^{-1}. The stability test was conducted at the potential of –0.23 V (*vs.* AgCl/Ag).

Figures

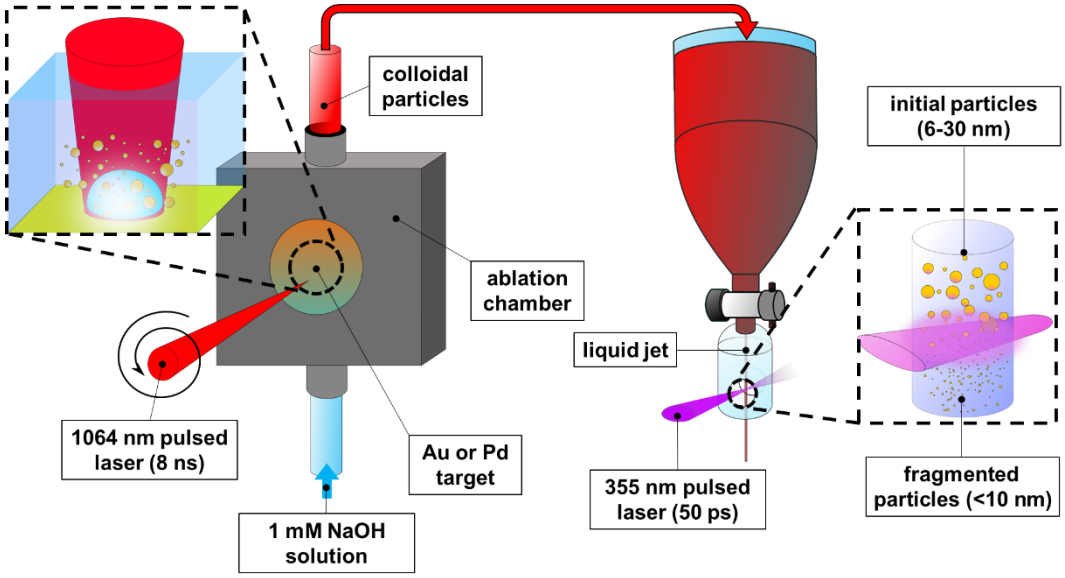

Figure S1. Schematic demonstration of the fabrication process of the metal NP colloids.

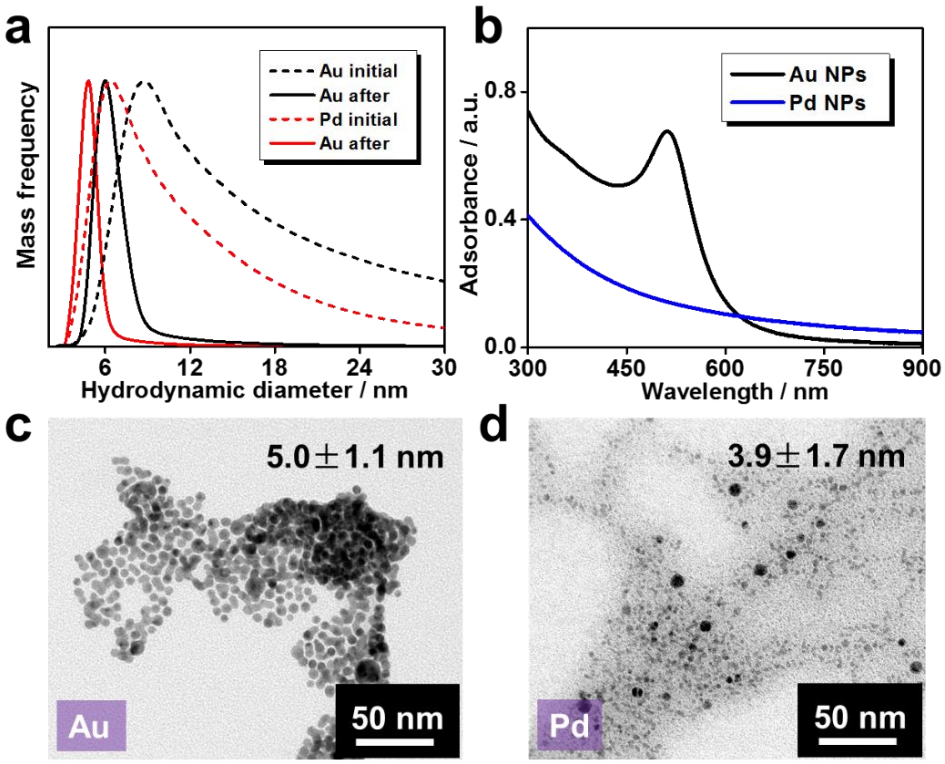

Figure S2. (a) The size distribution of the initially produced NPs by laser ablation and the NPs after laser fragmentation. (b) UV-vis absorption spectra and (c-d) TEM images of the finally used Au and Pd NPs.

Figure S3. Destabilization of (a) Au NPs, (b) Pd NPs, and (c) Au-Pd mixed NPs. For each photo, from left to right, showed the products as destabilized by $NaBH_4$, NH_4F, NH_4SCN, NaOH, and by heating at 50 ºC for 3 h. The concentration of all initiators is 100 mM. Gels were produced by $NaBH_4$ (for all three systems), as well as by NH_4F and NaOH (for the gold system).

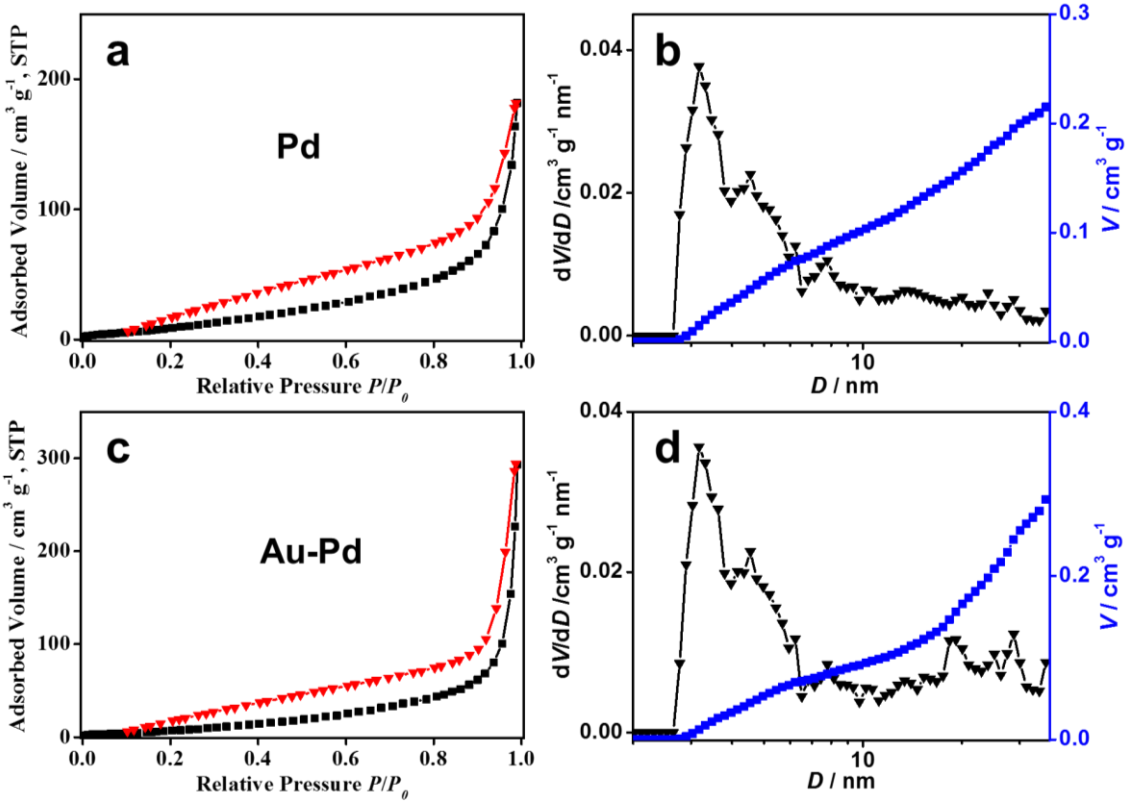

Figure S4. Nitrogen adsorption/desorption isotherms and the pore size distributions of the (a-b) Pd and (c-d) Au-Pd aerogels.

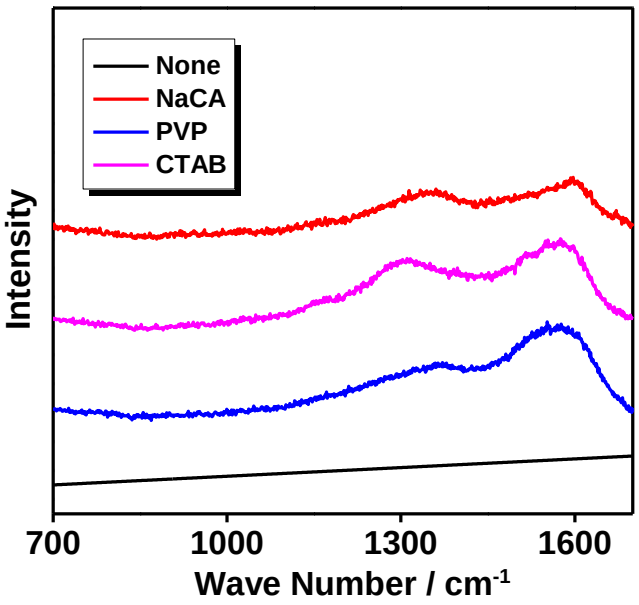

Figure S5. Raman spectra of the pristine Au-Pd and various ligand-modified Au-Pd aerogels.

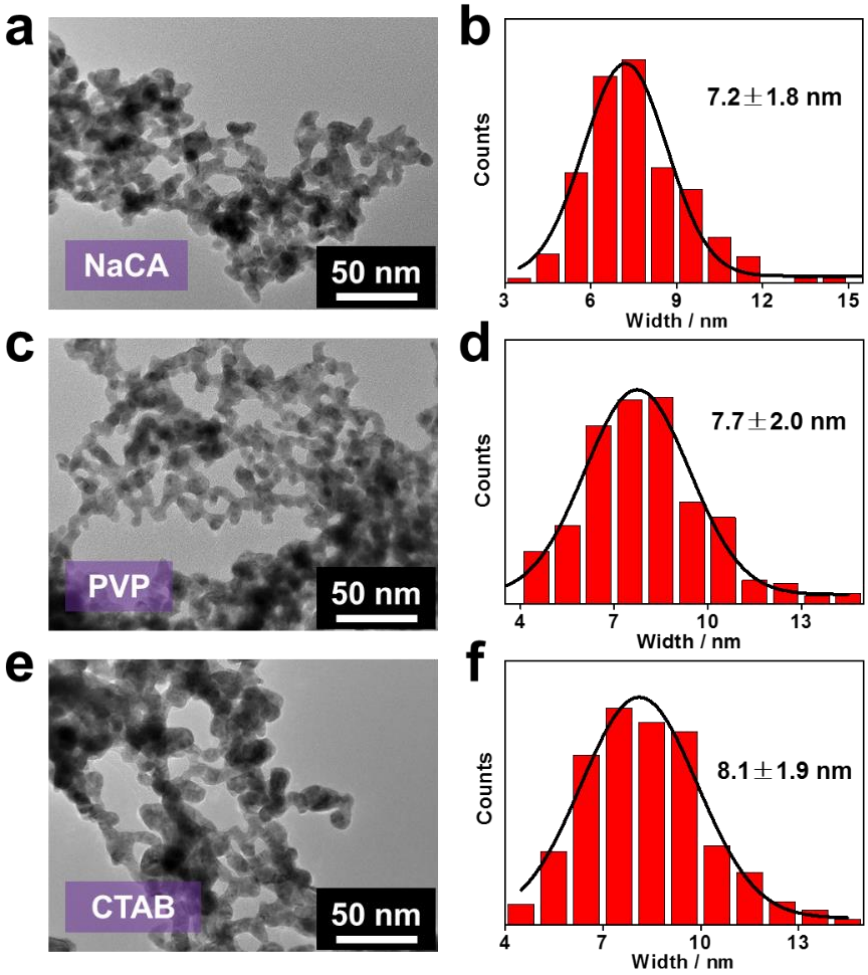

Figure S6. TEM images and the corresponding statistic ligament size distributions of various ligand-modified Au-Pd aerogels.

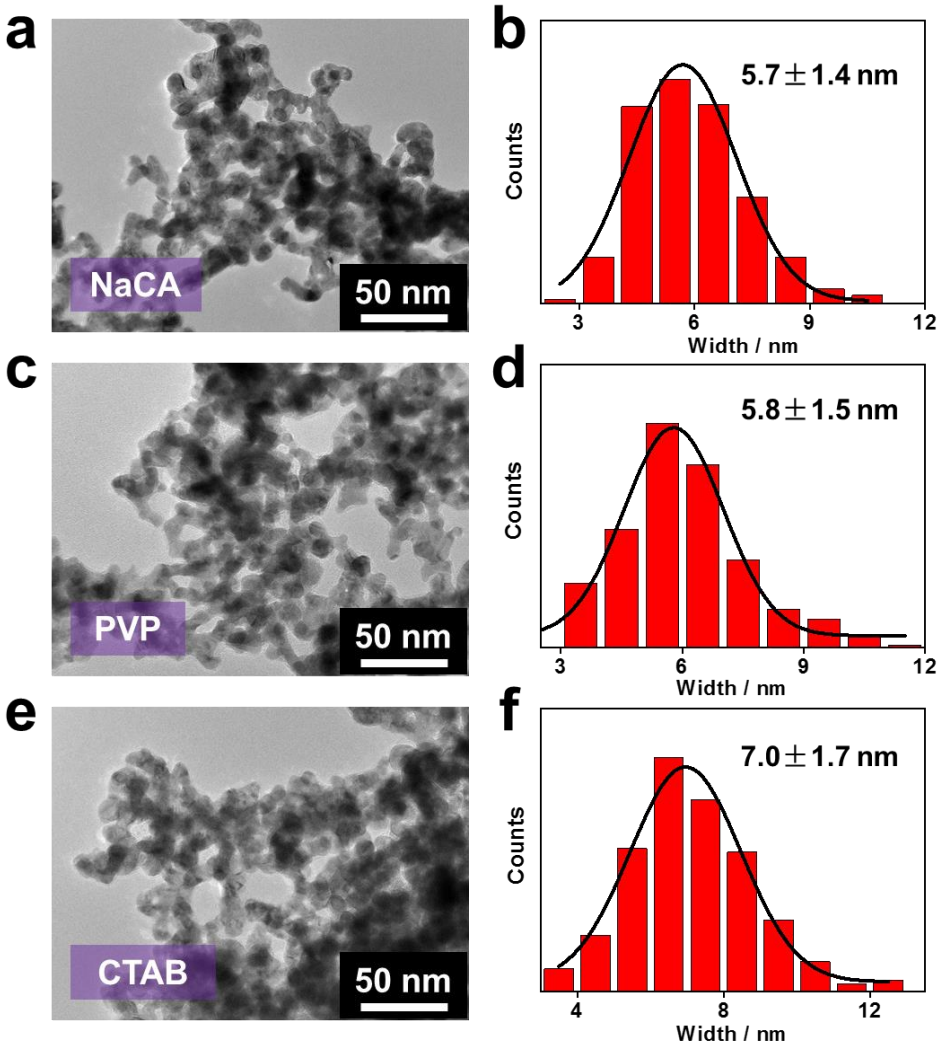

Figure S7. TEM images and the corresponding statistic ligament size distributions of various ligand-modified Pd aerogels.

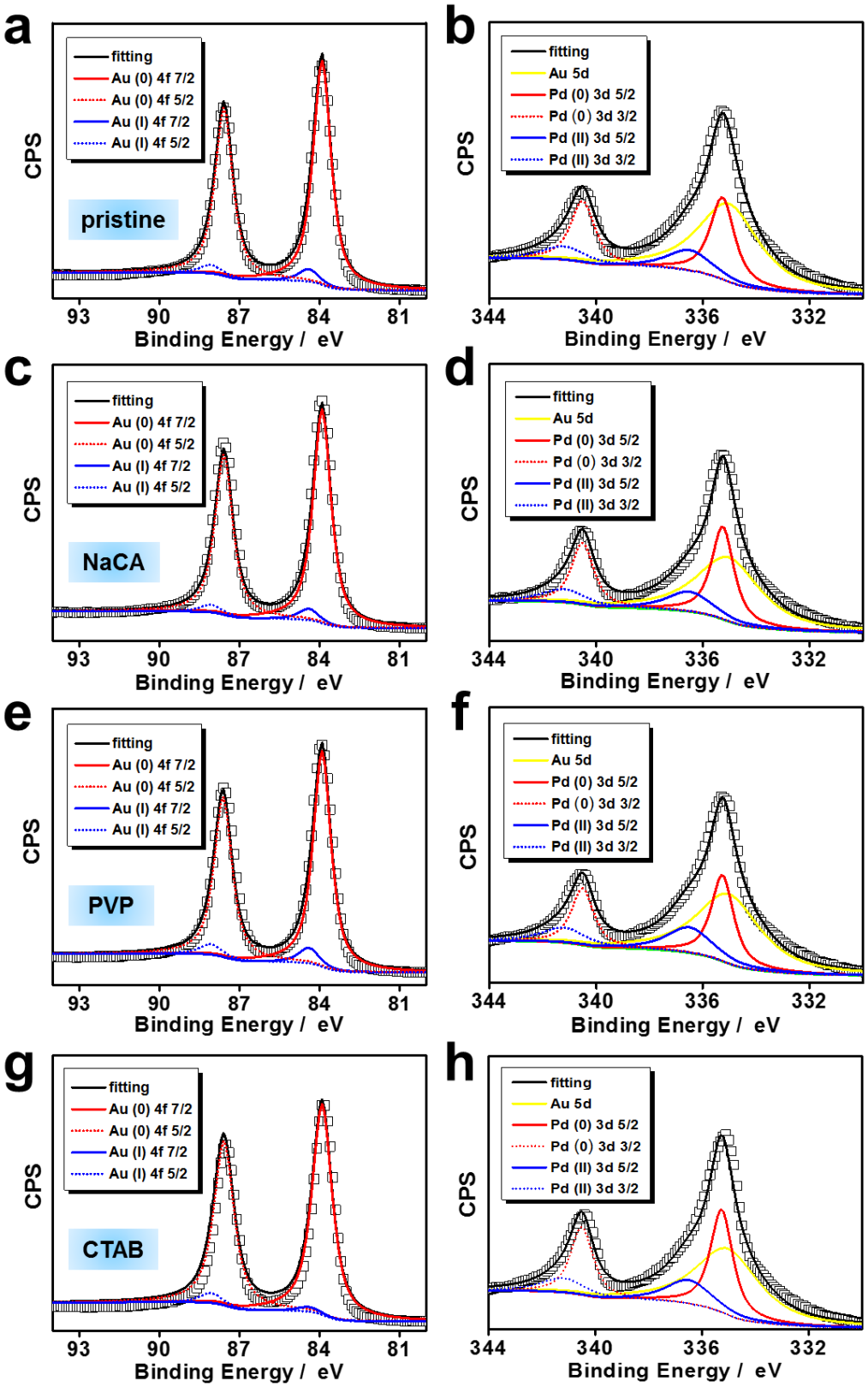

Figure S8. Deconvolution of the XPS Au 4f and Pd 3d spectra of (a-b) pristine, (c-d) NaCA-modified, (e-f) PVP-modified, and (g-h) CTAB-modified Au-Pd aerogels.

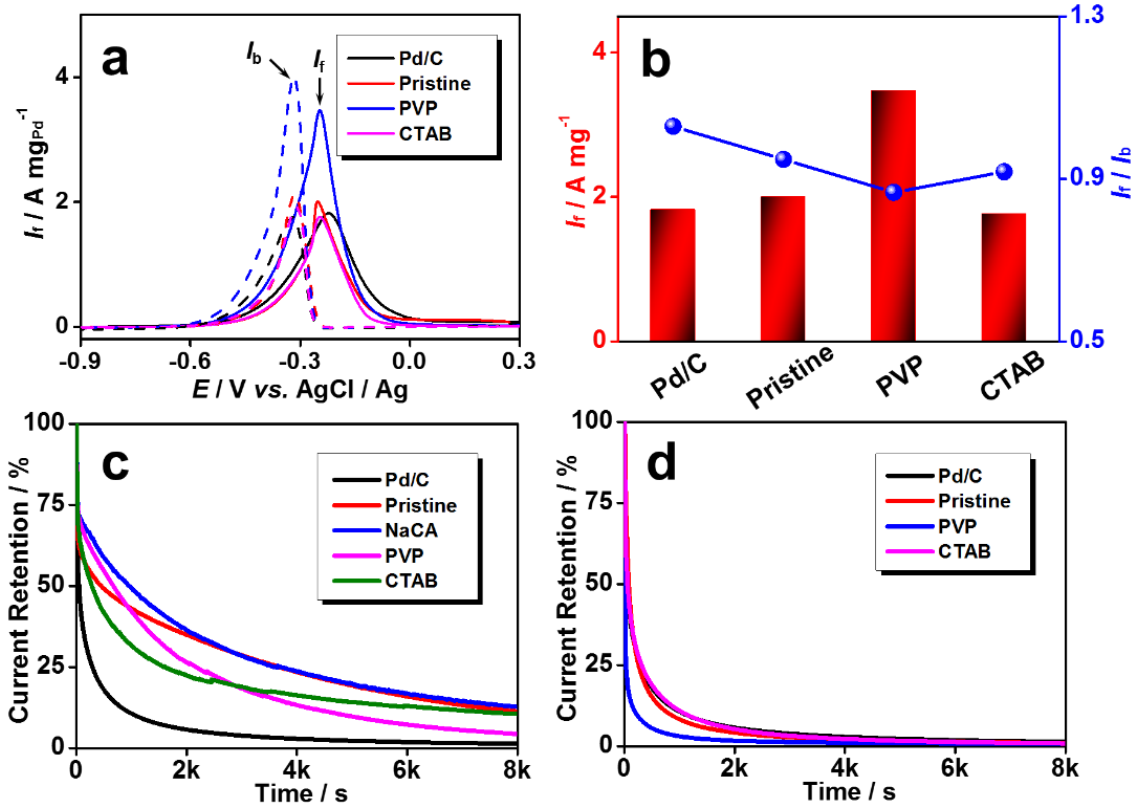

Figure S9. EOR performance of commercial and various aerogel catalysts. (a) CV curves and (b) summarized I_f and I_f/I_b. Current retention of Pd/C and (c) various ligand-modified Pd aerogels as well as (d) various ligand-modified Au-Pd aerogels. All tests were performed in nitrogen-saturated 1.0 M KOH + 1.0 M ethanol aqueous solution.

Tables

Table S1. Summary of nitrogen adsorption data and ligament sizes of the as-prepared aerogels. The specific surface area S_{BET} (m^2 g^{-1}) was calculated in the partial pressure (p/p_0) range of 0.1–0.3. The total pore volume V_{tot} is derived at p/p_0 = 0.99. The average ligament size d is derived from a statistic analysis of TEM measurements.

Metals	**Density / mg cm^{-3}**	**S_{BET} / m^2 g^{-1}**	**V_{tot} / cm^3 g^{-1}**	**d / nm**
Au	406.4	/	/	10.4 ± 3.1
Pd	77.9	61.1	0.281	5.9 ± 1.4
Au-Pd	77.3	47.7	0.453	6.8 ± 0.9

Table S2. The fraction of different-valence-state gold and palladium for pristine and various ligand-modified Au-Pd aerogels. The data were obtained from the deconvolution of the corresponding Au and Pd XPS spectra.

Sample	**Au (0)**	**Au (I)**	**Pd (0)**	**Pd (II)**
Pristine	94.0%	6.0%	68.4%	31.6%
NaCA	94.4%	5.6%	70.0%	30.0%
PVP	92.5%	7.5%	62.7%	37.3%
CTAB	97.5%	2.5%	72.0%	28.0%

References

1. R. Streubel, S. Barcikowski, B. Gökce, *Opt. Lett.* **2016**, *41*, 1486-1489.

2. A. R. Ziefuß, S. Barcikowski, C. Rehbock, *Langmuir* **2019**, *35*, 6630-6639.